R. Belitz, P. Meisner, M. Coeler, U. Wunderwald*, J. Friedrich, J. Zosel, M. Schelter, S. Jachalke and E. Mehner

Waste Heat Energy Harvesting by use of $BaTiO_3$ for Pyroelectric Hydrogen Generation

https://doi.org/10.1515/ehs-2016-0009

Abstract: The generation of hydrogen as a chemical energy storage for power generation via fuel cells or for the synthesis of fuels has attained a strong interest in recent years. By way of example this is realized using electrolysis of water with the help of excess electricity of wind power plants. However with low temperature grade waste heat as it could be found in many industrial and household applications, there is another source of usable energy for this purpose. In a first pragmatic experimentation we investigated the pyroelectric effect of ferroelectric $BaTiO_3$ combined with a temperature cycling to generate hydrogen from water. Therefore, single crystals ground to powder were brought into contact with distilled water and set to a cyclical temperature change from 40 °C to 70 °C. With the help of a highly selective and sensitive measuring system based on a coulometric solid electrolyte detector we could provide a first indication of pyroelectric generated hydrogen by a fraction of 300 Vol.-ppb in the sample gas.

Keywords: $BaTiO_3$, energy harvesting, hydrogen, pyroelectricity, waste heat

Introduction

The pyroelectric effect describes the coupling between a change of spontaneous polarization ($\Delta\vec{P_s}$) with respect to a temperature fluctuation (ΔT) of dielectric, crystalline matter, following the relation $\Delta\overrightarrow{P_S} = \vec{p}\,\Delta T$, in which the proportional factor $\vec{p}$ is the pyroelectric coefficient. The effect is known since ancient times, referenced in writings by Theophrastus in 314 BC (Caley and Richards 1956), however a widespread application took place in the mid-20th century with the development of infrared sensors using the occurrence of an electrical voltage arise from generated surface charges when exposed to heat.

Recent research work examined this effect on the antimicrobial effect on *Escherichia coli*, using perovskite type lithium niobate ($LiNbO_3$) and lithium tantalate ($LiTaO_3$) nano- and microcrystalline powder material (Gutmann et al. 2012), likely due to pyroelectrically generated reactive oxygen species (Benke et al. 2015). A further field of investigations is the application for ice repellent coatings on the basis of pyroelectric polyvinylidene fluoride (PVDF) reported by Spitzner et al. (2015). Xie et al. (2017) describe the water splitting by using an external pyroelectric charge source with thin films of lead zirconate titanate (PTZ) and polyvinylidene fluoride (PVDF). The application of the pyroelectric effect for hydrogen generation by water electrolysis in direct contact with water is described in several patent specifications towards process design and method of operation (Baldauf et al. 2012; Forman et al. 2015). But, the fundamentals of the water electrolysis process relating to the surface chemistry are still neither fully understood nor experimentally confirmed in literature. However, theoretical investigations for a possible mechanism of water electrolysis on ferroelectric $PbTiO_3$ single crystal were recently published by Kakekhani and Ismail-Beigi (2016). Experimental results for hydrogen generation are available for the application of the piezoelectric properties of ZnO fibers and $BaTiO_3$ dendrites, i. e. generating surface charges by applying mechanical stress via ultrasonic vibration to the material sample (Hong et al. 2010).

Due to its good chemical stability and adjustable ferroelectric properties $BaTiO_3$ (BTO) is the most intensively studied ferroelectric material for about six decades. In a temperature range between 5 °C to 120 °C the perovskite type structure is distorted by a shifted titanium ion outwards the center of the oxygen octahedra in the *z*-direction of the unit cell leading to the ferroelectric and with it pyroelectric tetragonal crystalline phase. The unit cell is characterized by a dipole moment with a surface potential on {001} surfaces, summarized to the spontaneous polarization.

***Corresponding author: U. Wunderwald,** Fraunhofer THM, 09599 Freiberg, Germany, E-mail: ulrike.wunderwald@thm.fraunhofer.de
R. Belitz, P. Meisner, M. Coeler, Fraunhofer THM, 09599 Freiberg, Germany
J. Friedrich, Fraunhofer THM, 09599 Freiberg, Germany; Fraunhofer IISB, 91058 Erlangen, Germany
J. Zosel, M. Schelter, Kurt-Schwabe-Institut für Mess- und Sensortechnik e.V. Meinsberg, 04736 Waldheim, Germany
S. Jachalke, E. Mehner, Institut für Experimentelle Physik, TU Bergakademie Freiberg, 09599 Freiberg, Germany

Experimental

Preparation of BTO Powder Material

BTO powder was prepared from commercially available single crystals (supplied by MaTecK) to get a form of the pyroelectric material that provides higher geometrical surface area than large chunks needed for the present experimental investigations. For this purpose irregular pieces of BTO single crystals were crushed and ground manually with an agate mortar and pestle to achieve a fine powder. Finally, single crystal particles with a maximum size of $d_P < 100\,\mu m$ were fractioned with a sieve. XRD analysis of the gained powder shows a good tetragonality, i. e. the splitting of the cubic 002 into 002 and 020 reflections (Figure 1).

Design of Hydrogen Generator

Due to its high fugacity as much as possible hydrogen should be generated pyroelectrically in a short time. To maximize the provided surface charges $\Delta Q = \Delta \overrightarrow{P_S} A$ with $\Delta \overrightarrow{P_S} = \vec{p}\,\Delta T$ the effective crystal surface area (A) and the value of temperature change (ΔT) are assessed as key process parameters in order to produce a large amount of hydrogen. Though the former was increased several orders of magnitude through the powder preparation. In contrast there is a strict limit for the upper temperature because of phase transition from the tetragonal to paraelectric cubic phase of BTO. Since, the hydrogen volume fraction of the sample gas is directly proportional to temperature change frequency a fast temperature change is much more important. Thus a fast heat transfer to and from the pyroelectric material is essential to facilitate short cycle times. This is accomplished by a small ashlar-formed container made of polystyrene (PS). The container is composed of two full-faced, square-cut sides with the dimensions $40 \times 40 \times 2\,mm^3$ and a frame with equal size and a cutout of approx. $25 \times 25\,mm^2$ and a material thickness of 2 mm. All parts were stacked on top of each other enclosing a void of about $1250\,mm^3$. Temperature is measured on the inside with a type K thermocouple. Two capillary tubes serve as N_2 inlet and outlet to the gas measuring system. Before the stack was glued together with cyanoacrylate, the void was filled loosely with a mass of 3.1 g BTO crystalline powder (Figure 2). Destilled water was filled into the container with the capillary tube as shown in Figure 4 after set up characterization (see below) before the test experiments.

Polarization of the Ferroelectric Material

In order to increase the net polarization of the $BaTiO_3$ particles, and thus maximize their pyroelectric activity, a

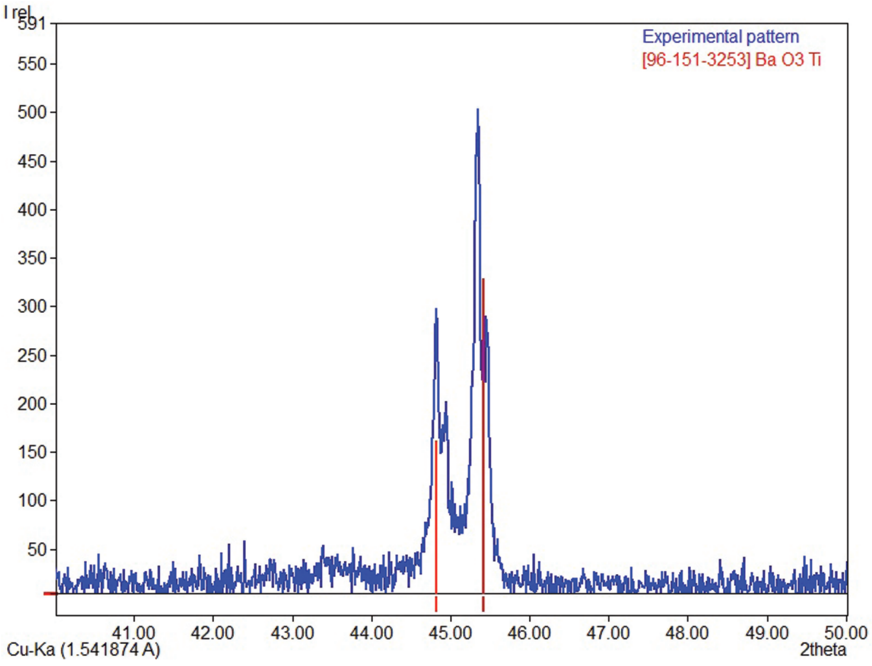

Figure 1: XRD analysis of the crystalline powder.

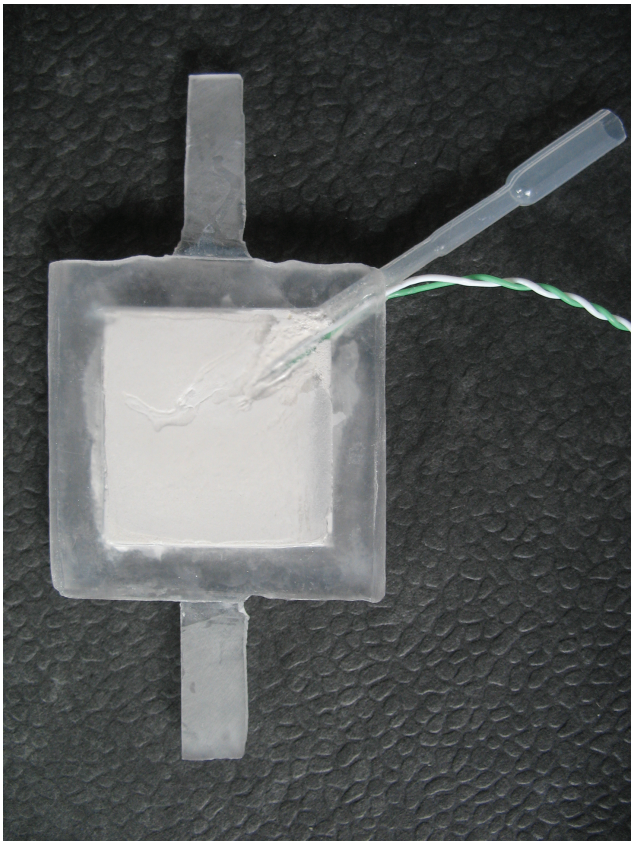

Figure 2: Picture of sandwiched container made of PS filled with polarized crystalline BTO powder, capillary tube and thermocouple, sticking in the container (External dimension of the container $40 \times 40 mm^2$).

polarization procedure, i. e. the application of an electric field above the coercive field strength of the material, is required for a parallelization of the randomized dipole moments. To minimize arcing, the material was poled in vacuum between two parallel stainless steel plates, to avoid contamination by the conventional "oil poling technique". Assuming a coercive field strength of $E_C = 0.35\,MV/m$ for single crystals (Shieh et al. 2009), a minimal voltage of 1.75 kV with a plate distance of 5 mm is necessary for polarization reversal. Thus, the powder filled container was poled at 2 kV for approx. 15 min.

Design of Experimental Set-up

To subject the pyroelectric material to a fast temperature cycling we decide to move the sample material between an hot and cold reservoir instead of switching between cooling and heating of the static device. Figure 3 shows the design of the test setup. Due to their high heat power density we use four Peltier heat pumps, two of them with the hot side opposite to each other as heat source and the other with the cold side opposite to each other for cooling the filled container. To ensure best operation mode (i. e. backside ambient temperature) the Peltier elements were equipped additionally with four heat dissipators and fans. The whole setup was fixed in a support frame assembled from aluminum profiles.

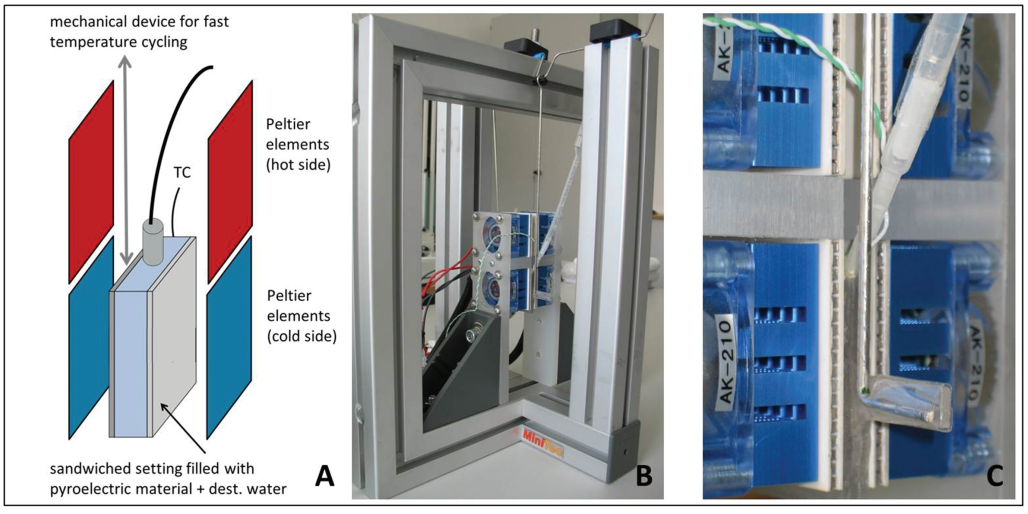

Figure 3: Scheme of the sandwiched container (see Figure 4) positioned within Peltier elements (A) and picture of the experimental set-up (B), with enlarged detail (C) showing container between lower cooling Peltier elements with capillary tube for the gas measuring system.

During the experiment the filled container was easily moved up and down manually using a crank with connecting rods.

Characterization of Temperature Cycling

The experimental procedure started with the characterization of the temperature cycling. After steady-state was attained for the upper and lower temperature level with the help of the Peltier elements, the container was set between the upper heating elements until equalization. Then, the temperature cycling started waiting to reach the preset temperature at each reversal point. This yields to large cycle duration of 7 min between 25 °C and 66 °C, which could be reduced by changing the containers position before maximum resp. minimum temperature was reached inside as shown in Figure 4. Keeping the presetting of current resp. voltage of the Peltier elements constant with higher frequency of the cycling of the container, there is either the favored fast temperature change between 35 °C and 56 °C, but low ΔT or the favored high ΔT between 45 °C and up to 90 °C, but slow temperature change inside the container. For the experimentation with hydrogen generation and gas analyzing we choose a periodic temperature change from 40 °C to 70 °C (ΔT = 30K) and duration of one cycle of 2 min (f = 8,3mHz) as a good compromise out of it.

After the basic characterization of the temperature cycling the container was filled with distilled water and put into the test setup for carrying out the tests.

Gas Analyzer for Hydrogen Detection

With help of a highly selective and sensitive measuring system, hydrogen and oxygen can be detected with lower limits of about 50 Vol.-ppb. Figure 5 shows a schematic of the measuring system, consisting of a sample injection port, gas chromatographic columns and a solid-electrolyte cell acting as detector (Schelter et al. 2013). The gaseous sample is injected into a carrier gas flow of the gas chromatograph (MG1 from SRI Instruments Europe GmbH, Bad Honnef, Germany) by using a sampling loop with a volume of 1 ml. Two packed columns, one with silica gel and one with a molecular sieve, provide the separation of the components such as hydrogen, oxygen and water vapour within 5 min at 50 °C column temperature in Ar carrier-gas flow of 20 ml/min.

The coulometric detector used in this work consists of a heated tube made of yttria-stabilized zirconia (8 mol-% yttria) with the outer diameter 5.7 mm and a wall thickness 1 mm. The tubular platinum electrodes on the inner and the outer surface of this tube are 60 mm in length. Between the working (inner) and the reference (outer) electrode a constant potential of −450 mV was applied by a self-made potentiostat, where the measuring gas is flowing through the tube while air serves as reference gas.

The principle of the coulometrically operated solid electrolyte detector is based on the complete oxidation or reduction of the gas component to be measured at the working electrode of a solid electrolyte cell heated to 650 °C resulting in an electronic current.

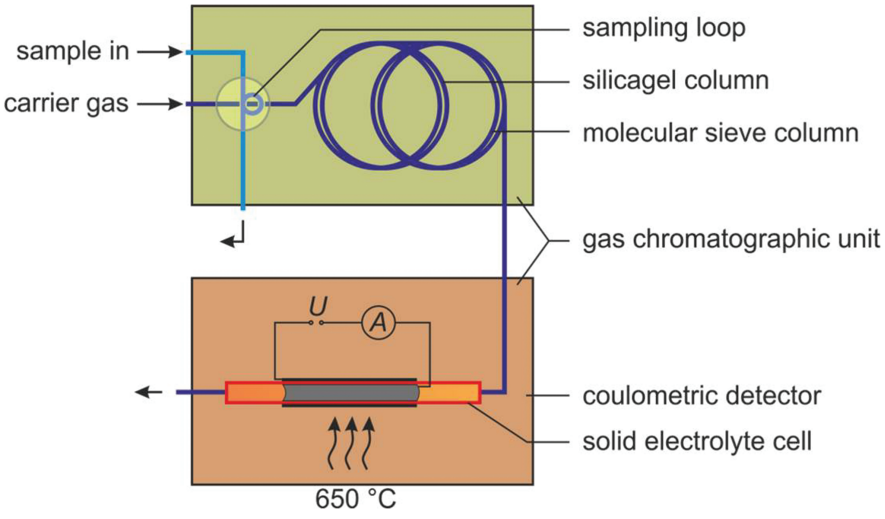

Figure 4: Temperature profile by cycling the container between lower cooling and upper heating Peltier elements.

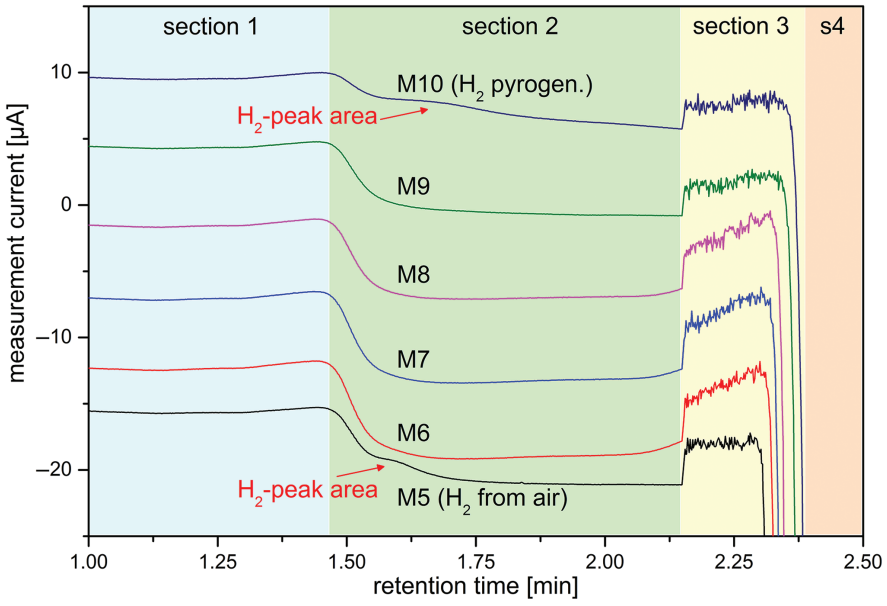

Figure 5: Schematic viewgraph of the measuring system consisting of a sample injection system, gas chromatographic columns and a coulometric solid electrolyte detector.

Figure 6 shows results of the determination of the detection limit of the measuring system for hydrogen. The measuring gas is a mixture of H_2 and N_2 adjusted by mass flow controllers (Brooks Instrument Company, Hatfield, USA). The determined detection limits, marked by dashed lines, show that in the sub-ppm concentration range the peak height h is a more accurate measure than the peak area A. Those two variables are determined by equation (I) and (II). The equations involve the measured current signal of the gas chromatograph $I(t)$ and the linear baseline function $I_b(t) = m^*t + n$. The baseline function is determined by choosing two points in the chromatogram, one of them at the time t_1 before the hydrogen peak and one at t_2 shortly after this peak.

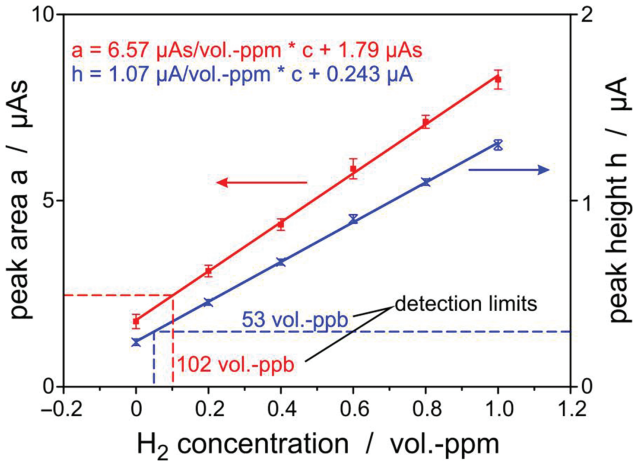

Figure 6: Results for the detection limit of the measuring system for hydrogen (Schelter et al. 2013).

(I) Peak height: $h = max\ (I(t) - I_b(t))$

(II) Peak area: $A = \int_{t1}^{t2} (I(t) - I_b(t))\ dt$

Proof of Hydrogen Generation

Before the start of the temperature cycling, a first measurement of the gas phase was done. Figure 7, shows 6 different measurements of the gas analyser. The curve progression for the measurements M5 – M10 shows at first the incoming baseline (Section 1). The relatively constant level of this baseline is mainly determined by the oxygen traces in the carrier gas of the chromatographic separation. In Section 2 this baseline shift to more negative currents is caused most probably by oxygen from the injected sample which is not retended in the column due to oxygen overload by the injected sample. Then a sharp shift in Section 3 occurs due to a switching between two current measuring ranges which are three orders of magnitude distant of each other (25 µA, 25 mA). The noise is more pronounced and a tiny deviation between the two ranges causes the shift of the baseline. At the end sharp bend to negative current increase (Section 4). This is caused by the beginning of the large oxygen peak in the sample. The curve labeled with measurement No. M5 and with the H_2 peak area shows with residual hydrogen from ambient air still contained in the overall system. Hence a purge with nitrogen was done for several minutes. Meanwhile further measurements were done (M6 ... M8) until no more hydrogen was detected.

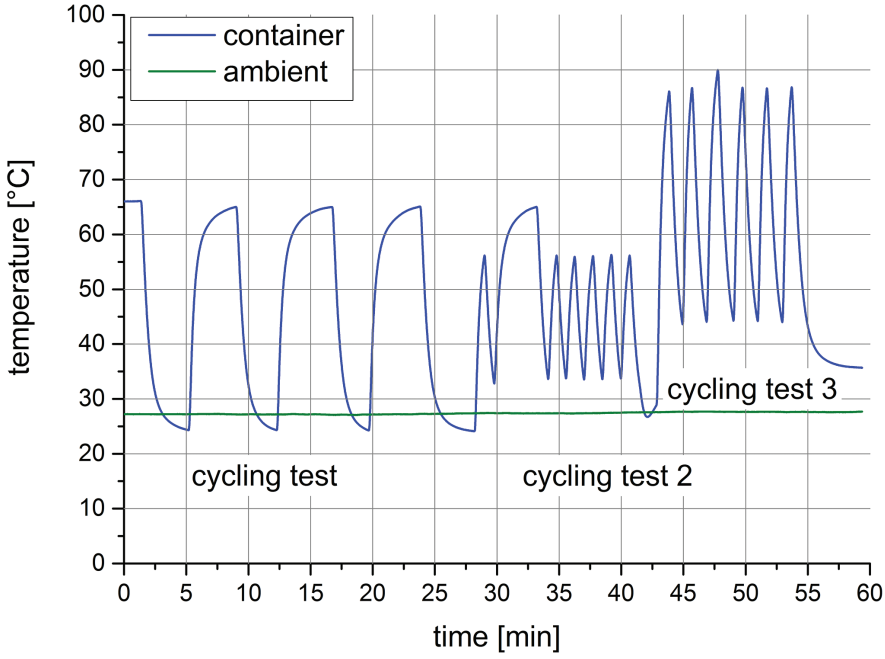

Figure 7: Proof of pyroelectric hydrogen generation with a highly selective measuring system with coulometric solid electrolyte detector.

Then temperature cycling started again and after a few cycles a volume fraction of hydrogen of 300 Vol.-ppb in the sample gas was detected (measurement No. M10 and labeled H_2 peak area), which is attributed to pyroelectric water electrolysis. The hydrogen concentration in the sample is calculated from the peak area (see picture) of the hydrogen peak and the sample loop volume using the Faraday law with a sample loop volume of 0.95 ml and a peak area of 2 µAs (Schelter et al. 2013).

Conclusions

We have investigated the applicability of for direct pyroelectric hydrogen generation in principle. For this purpose commercially available $BaTiO_3$ single crystals were manually ground to powder and proven to be in the tetragonal phase by XRD. After a polarization procedure to the powder to parallelize the randomly oriented dipole moments and thus increase the pyroelectric functionality, the $BaTiO_3$ particles were enclosed into a small container with distilled water and exposed to a cyclical temperature change. The container was set to a cyclical temperature change from 40 °C to 70 °C with resulting ΔT of 30 K and duration of one cycle of 2 min.

Using a highly sensitive measuring system with a solid electrolyte detector we could provide a first indication, showing 300 Vol.–ppb of pyroelectrical generated hydrogen.

Although, these results were obtained with a simple test-setup, they offer essential prove of concept that pyroelectric materials may be used to generate hydrogen from water with the help of low grade waste heat. For a subsequent technical implementation there is still more research required especially regarding other pyroelectric materials.

References

Baldauf, M., T. Hammer, S. Kosse, and G. Zimmermann. 2012. "Device for Splitting a Chemical Compound and Associated Method." Patent WO2012/110352A1.

Benke, A., E. Mehner, M. Rosenkranz, E. Dmitrieva, T. Leisegang, H. StöCker, W. Pompe, and D. C. Meyer. 2015. "Pyroelectrically Driven •OH Generation by Barium Titanate and Palladium Nanoparticles." *Journal Physical Chemical C* 119:18278.

Caley, E. R., and J. F. C. Richards, eds. 1956. *Theophrastus: On Stones*, Columbus: Ohio State University.

Forman, C., M. Gootz, D. Scheithauer, M. Herrmann, E. Mehner, B. Meyer, D. C. Meyer, I. Muritala, R. Pardemann, O. Schulze, and T. Leisegang. 2015. "Vorrichtung und Verfahren zur Energie-und Stoffwandlung mittels pyroelektrischer Materialien zur Herstellung von Spaltprodukten." *Patent DE102014003815A1.*

Gutmann, E., A. Benke, K. Gerth, H. Böttcher, E. Mehner, C. Klein, U. Krause-Buchholz, U. Bergmann, W. Pompe, and D. C. Meyer. 2012. "Pyroelectrocatalytic Disinfection Using the Pyroelectric Effect of Nano- and Microcrystalline LiNbO3 and LiTaO3 Particles." *Journal Physical Chemical C* 116:5383.

Hong, K.-S., H. Xu, H. Konishi, and X. Li. 2010. "Direct Water Splitting through Vibrating Piezoelectric Microfibers in Water." *Journal Physical Chemical Letters* 1:997.

Kakekhani, A., and S. Ismail-Beigi. 2016. "Ferroelectric Oxide Surface Chemistry: Water Splitting via Pyroelectricity." *Materials Chemical A* 4:5235.

Schelter, M., J. Zosel, W. Oelßner, U. Guth, and M. Mertig. 2013. "A Solid Electrolyte Sensor for Trace Gas Analysis." *Sensors and Actuators B: Chemical* 187:209.

Shieh, J., J. H. Yeh, Y. C. Shu, and J. H. Yen. 2009. "Hysteresis Behaviors of Barium Titanate Single Crystals Based on the Operation of Multiple 90° Switching Systems." *Material Science and Engineering B* 161:50.

Spitzner, D., U. Bergmann, S. Apelt, R. A. Boucher, and H.-P. Wiesmann. 2015. "Reversible Switching of Icing Properties on Pyroelectric Polyvenylidene Fluoride Thin Film Coatings." *Coatings* 5:724.

Xie, M., S. Dunn, E. Le Boulbar, and C. R. Bowen. 2017. "Pyroelectric Energy Harvesting for Water Splitting." *International Journal of Hydrogen Energy*. doi:10.1016/j.ijhydene.2017.02.086.